Enhanced Parameter Identification of Solar Photovoltaic Models Using a Novel Two-Stage Improved Sea Lion Optimization Algorithm

Zhanghao Chen*, Kun-Che Ho**‡, Yi-Hua Liu***

* Ascend Trading & Consultation (Shenzhen) Co., Ltd, Room 401, Building B, Fu'an Technology Building, No. 013, Gaoxin South 1st Road, High-tech Zone Community, Yuehai Street, Nanshan District, Shenzhen 518000, China

** Department of Automation Engineering, National Formosa University, No.64, Wunhua Rd., Huwei Township, Yunlin County 632301, Taiwan

*** Department of Electrical Engineering, National Taiwan University of Science and Technology, No. 43, Sec. 4, Keelung Rd., Da'an Dist., Taipei City 106335, Taiwan

(c.zhanghao@163.com, kcho@nfu.edu.tw, yhliu@mail.ntust.edu.tw)

‡ Corresponding Author; Kun-Che Ho, No.64, Wunhua Rd., Huwei Township, Yunlin County 632301, Taiwan, Tel: +886 631 5386, kcho@nfu.edu.tw

Received: 06.05.2025 Accepted: 23.06.2025

Abstract- This study introduces a novel two-stage metaheuristic framework for parameter identification (PI) of the single diode model (SDM) in solar cells. The Sea Lion Optimizer (SLO) is, for the first time, applied to SDM parameter estimation and compared with five other classical and recent metaheuristic algorithms. Results demonstrate SLO's superior performance. An improved SLO (ISLO) is then developed, incorporating Lévy flight and personal best information to enhance accuracy. To further improve the accuracy, a two-stage methodology is proposed, using mathematical analysis of the SDM to derive initial parameter estimates and refine search ranges. This approach significantly enhances parameter estimation accuracy and robustness. ISLO shows enhanced accuracy, with an overall RMSE improvement of approximately 59.7 % compared to SLO. The two-stage ISLO further improves estimation, reducing the mean and standard deviation of RMSE by 89.6 % and 91.3 %, respectively. The proposed two-stage method can also be integrated with other metaheuristic algorithms for similar gains.

Keywords- Photovoltaic model, parameter identification, metaheuristic optimization, sea lion optimizer, two-stage method.

1. Introduction

Photovoltaic (PV) systems play a pivotal role in global renewable energy generation due to their scalability, declining cost, and potential for carbon emission reduction. The reliable operation and accurate performance modeling of PV systems are therefore critical for optimizing energy yield and ensuring grid stability in modern power systems. Previous research has demonstrated the effectiveness of advanced techniques in related power system domains, including fuzzy logic-based transformer protection [1] and harmonic analysis for insulator reliability studies [2]. These approaches underscore the value of sophisticated analytical methods for addressing critical electrical system challenges, motivating our investigation of SDM PI in PV systems. PI techniques for PV models are critical for accurately simulating and optimizing the performance of PV systems. These techniques extract key parameters, such as photocurrent, diode ideality factors, and resistances, from PV models like the single diode model (SDM), double diode model (DDM), and triple diode model (TDM). PI methods for PV model can be classified into analytical, numerical/iterative, and meta-heuristic approaches. Each category offers distinct advantages and challenges, as discussed below. Analytical methods use deterministic equations derived from PV datasheet values to estimate parameters. These methods are computationally efficient and rely on mathematical formulations to compute parameters directly. Brano et al. [3] developed an improved five-parameter model for SDM, incorporating temperature and irradiance effects for enhanced accuracy. Orioli and Di Gangi [4] advanced this approach by eliminating the need for graphical data, streamlining computations. Lineykin et al. [5]

employed Kirchoff's laws and the Lambert W function to achieve precise parameter estimation. While analytical methods are fast and straightforward, their accuracy can be limited under varying environmental conditions due to simplifying assumptions, making them less adaptable to complex scenarios. Numerical and iterative methods utilize computational algorithms to solve nonlinear equations, offering greater accuracy by iteratively refining parameter estimates to minimize errors between modeled and measured I-V curves. Calasan et al. [6] proposed an iterative approach using the Lambert W function for DDM and TDM, achieving high precision in parameter extraction.

Similarly, Calasan et al. [7] conducted a comparative analysis of iterative methods, highlighting their reliable convergence for complex models. Silva et al. [8] introduced a parameter estimation method to improve PV model accuracy, emphasizing numerical robustness. These methods provide high accuracy but are computationally intensive and may encounter convergence challenges, particularly for multi-diode models. Meta-heuristic methods employ soft computing algorithms to optimize parameter extraction by minimizing objective functions, making them highly effective for complex models. These probabilistic approaches excel in handling nonlinear and multimodal problems. Qais et al. [9] utilized a novel circle search algorithm for TDM, demonstrating superior accuracy and robustness. Soliman et al. [10] applied the equilibrium optimizer algorithm, while Gafar et al. [11] used modified spotted hyena optimization, both achieving precise results across diverse conditions. Meta-heuristic methods are versatile and accurate but require significant computational resources and expertise to tune algorithm parameters, posing challenges for real-time applications. Table 1 summarizes the advantages and disadvantages of these methods.

Table 1. The pros and cons of different type of PI methods

Method	**Advantages**	**Disadvantages**
Analytical	Fast, simple, low computational demand	Limited accuracy, sensitive to conditions
Numerical/iterative	High accuracy, reliable convergence	Computationally intensive, convergence issues
Meta-heuristic	Robust, versatile, high accuracy	High computational cost, complex tuning

Meta-heuristic (MH) algorithms have been extensively employed to address various engineering challenges, demonstrating superior performance in multiple applications. Notable implementations include energy storage optimization using GA and PSO for smart grid peak shaving [12], stochastic unit commitment with hybrid techniques for cost-emission reduction [13], and reliability-cost balanced sizing of hybrid renewable systems [14]. Additional applications encompass optimal DG and capacitor placement via artificial bee colony algorithms [15], stability enhancement through coordinated controller optimization [16], and multi-objective microgrid operation management [17].

Given these demonstrated successes, this study proposes to adopt MH methods for SDM parameter identification (PI). Meta-heuristic methods have gained significant popularity for PI of the SDM in PV systems due to their ability to address the complex, nonlinear, and multimodal nature of the optimization problem involved. The SDM, which models PV modules using parameters like photocurrent, reverse saturation current, diode ideality factor, series resistance, and shunt resistance, requires precise parameter extraction to accurately represent the I-V characteristics under varying environmental conditions. In addition, meta-heuristic methods offer versatility across different PV models and operating conditions. These methods can be applied to SDM, DDM, and TDM with minimal adjustments, as demonstrated by algorithms like differential evolution [18-20] and particle swarm optimization [21-23]. For SDM, this adaptability is crucial because PV modules operate under varying irradiance and temperature conditions, which affect parameter values. Moreover, the significant increase in computational power has made meta-heuristic methods more practical. Algorithms like genetic algorithms (GA) [24-26], artificial bee colony optimization [27-29], and whale optimization [30-32] require substantial computational resources due to their population-based search mechanisms. However, modern workstations and parallel computing architectures, as referenced in [33], have reduced this barrier, enabling faster execution of these algorithms. This computational feasibility has driven their adoption for SDM parameter identification, where high accuracy justifies the resource investment. Finally, meta-heuristic methods provide high accuracy and robustness, which are critical for real-world PV applications. The document highlights that algorithm like the Harris Hawks optimization [34] and marine predators' algorithm [35-36] achieve precise parameter estimates by minimizing error metrics effectively. For SDM, this precision translates to better performance prediction, improved maximum power point tracking, and enhanced system design, which are vital for optimizing renewable energy systems.

This study presents a new two-stage metaheuristic framework for addressing the parameter identification (PI) problem in the SDM, offering distinct improvements over existing methods. For the first time, the Sea Lion Optimizer (SLO) algorithm is applied to SDM parameter estimation. The SLO's performance is evaluated against established algorithms, such as GA and Grey Wolf Optimizer (GWO), as well as recent methods, including Coati Optimization Algorithm (COA), African Vulture Optimization Algorithm (AVOA), and Golden Jackal Optimizer (GJO). Results show that SLO performs better than these alternatives.

To improve estimation accuracy, an Improved SLO (ISLO) is developed by incorporating Lévy flight and personal best information. This leads to a 59.7% reduction in Root Mean Square Error (RMSE) for SDM parameter identification compared to the original SLO. Additionally, to address the sensitivity of MH algorithms to initial conditions and search boundaries, a two-stage approach is proposed.

In the first stage, a mathematical analysis of the SDM provides initial parameter estimates. These are used in the second stage to set narrower search ranges for the MH algorithm. This method improves accuracy and robustness, with ISLO achieving 89.6% and 91.3% reductions in the mean and standard deviation of RMSE, respectively.

The proposed framework is adaptable and can be applied to other MH algorithms to enhance their performance, unlike methods in prior studies. The main contributions of this work are:

- SLO Application: The first use of SLO for PV model parameter estimation, outperforming existing MH algorithms.
- ISLO Development: An enhanced ISLO with Lévy flight and personal best information, reducing RMSE by 59.7% compared to the original SLO.
- Two-Stage Framework: A methodology using mathematical analysis and refined search ranges, achieving 89.6% and 91.3% reductions in mean and standard deviation of RMSE, respectively, and applicable to other MH algorithms.

Figure 1 illustrates the schematic diagram of each research phase presented in this study.

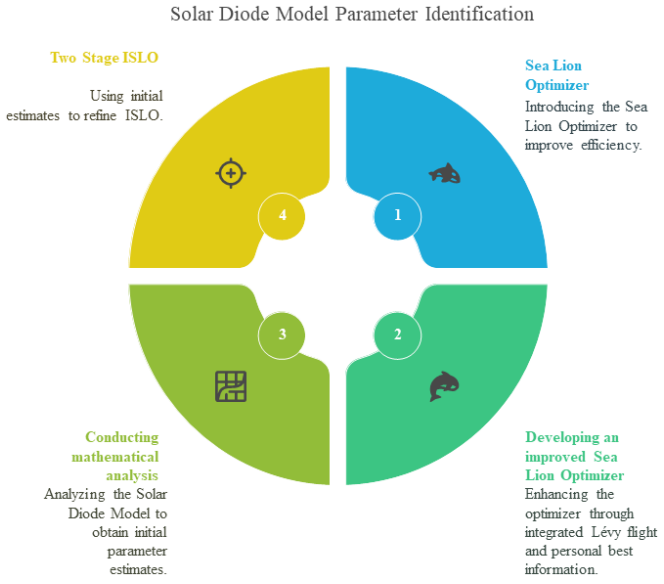

Fig. 1. Schematic diagram of each research phase of this study.

1.1. Nomenclature

Symbols

C_0: Scaling constant for diode saturation current
E_g: Bandgap energy of the semiconductor material (eV)
I_{MPP}: Current at Maximum Power Point (A)
$I_{exp,i}$: Measured current at the i-th data point (A)
I_{ph} / I_{ph0}: Photogenerated current (A)
I_{pv}: Output current of the PV model (A)
I_{sd} / I_0 / I_{S0}: Diode saturation current (A)
$I_{sim,i}$: Simulated current at the i-th data point (A)
I_{SC} / I_{SC0}: Short-circuit current (A)
k: Boltzmann constant (1.3806×10^{-23} J/K)
Lévy(s): Lévy step vector in D-dimensional space
m: Random number in the range [−1, 1]
n / n_0: Diode ideality factor (dimensionless)
N: Number of data points
N(0,1): Standard normal distribution
q: Electron charge (1.602×10^{-19} C)
r, r_1, r_2, r_3, r_4: Random numbers in the range [0, 1]
R_{sh} / R_{sh0}: Shunt resistance (Ω)
RMSE: Root Mean Square Error
R_S / Rs_0: Series resistance (Ω)
ss: Step size for Lévy flight
T / T_0: Temperature (K) / Reference temperature (K)
V_{MPP}: Voltage at Maximum Power Point (V)
V_{OC} / V_{OC0}: Open-circuit voltage (V)
X: Parameter vector [I_{ph}, I_{sd}, n, R_s, R_{sh}]
α_{Isc}: Temperature coefficient of short-circuit current (%/°C)
β_{Voc}: Temperature coefficient of open-circuit voltage (%/°C)
θ, ϕ: Angles of voice reflection and refraction (radians)
⊗: Element-wise (entry-wise) multiplication operator

Abbreviations

ABC: Artificial Bee Colony
AVOA: African Vulture Optimization Algorithm
COA: Coati Optimization Algorithm
DDM: Double diode model
DG: Distributed Generation
GA: Genetic Algorithm
GJO: Golden Jackal Optimizer
GWO: Grey Wolf Optimizer
ISLO: Improved Sea Lion Optimizer
MAE: Mean Absolute Error
MH: Meta-heuristic
PI: Parameter Identification
PV: Photovoltaic
RMSE: Root Mean Square Error
SDM: Single Diode Model
SLO: Sea Lion Optimizer
STC: Standard Test Conditions
TDM: Triple diode model

2. Single Diode Model and Parameter Extraction Problem

SDM as shown in Figure 2 is a widely adopted equivalent circuit model used to describe the current-voltage (I-V) characteristics of PV cells and modules. This model consists of a current source representing the photogenerated current (I_{ph}), a diode accounting for recombination losses, a series resistance (R_s) modeling ohmic losses, and a shunt resistance (R_{sh}) representing leakage current. The SDM provides a good compromise between simplicity and accuracy, making it suitable for PV system analysis and optimization.

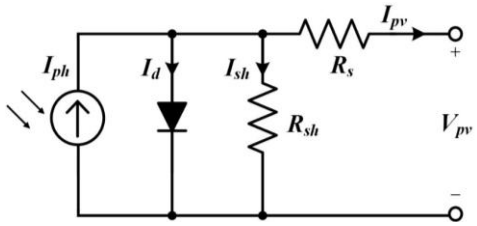

Fig. 2. Schematic of a single diode model.

The output current (I_{pv}) of the SDM is governed by a nonlinear equation that combines these components. The mathematical representation is given by:

$$I = I_{ph} - I_{sd}\left(\exp\left(\frac{q(V+IR_s)}{nkT}\right)-1\right)-\frac{V+IR_s}{R_{sh}} \quad (1)$$

Here, I_{ph} is the photogenerated current, I_{sd} is the diode saturation current, q is the electron charge (1.602×10^{-19} C), n is the diode ideality factor (typically between 1 and 2), k is the Boltzmann constant (1.3806×10^{-23} J/K), T is the temperature in Kelvin, R_s is the series resistance, and R_{sh} is the shunt resistance.

Extracting the five unknown parameters (I_{ph}, I_{sd}, n, R_s, and R_{sh}) from experimental I-V data is a challenging task due to the nonlinear and implicit nature of the equation. Traditional analytical methods often require good initial guesses and may converge to local minima. To overcome these limitations, metaheuristic optimization methods are employed in this study. These methods efficiently explore the parameter space without requiring initial estimates and are robust against measurement noise. The optimization process involves minimizing the RMSE between the experimental and simulated current values. The RMSE is defined as:

$$RMSE(X) = \sqrt{\frac{1}{N}\sum_{i=1}^{N}(I_{exp,i} - I_{sim,i}(X))^2} \quad (2)$$

where N is the number of data points, $I_{exp,i}$ is the measured current at the i-th data point, and $I_{sim,i}$ is the current predicted by the SDM for a given parameter set X = [I_{ph}, I_{sd}, n, R_s, R_{sh}].

3. The Compared Metaheuristic Methods in This Study

This study proposes the use of the SLO for PI of the SDM, and evaluates its estimation performance in comparison with several other MH algorithms, including GA, GWO, COA, AVOA, and GJO. Section 3.1 presents the SLO employed in this work, while Section 3.2 reviews the MH-based SDM parameter extraction methods reported in the literature.

3.1. Description of Basic SLO

The SLO is Introduced by Raja Masadeh et. al. in 2019, it is a nature-inspired MH optimization algorithm that mimics the hunting behavior of sea lions in the wild [37]. SLO involves the following main phases:

Step 1 Initialization: The algorithm begins by creating a population of sea lions, where each sea lion represents a potential solution to the optimization problem. To achieve this, the position of each sea lion is initialized randomly within the search space. This initialization process uses the equation:

$$X_{i,j}^{init} = X_{i,j}^{min} + rand_{i,j}(X_{i,j}^{max} - X_{i,j}^{min}) \quad (3)$$

Here, $X_{i,j}^{init}$ represents the initial position vector of the i-th solution, $X_{i,j}^{min}$ and $X_{i,j}^{max}$ define the minimum and maximum boundaries for the j-th dimension of the i-th solution, and rand is a uniform random value selected from the interval [0, 1].

Step 2 Detecting and Tracking Phase: In this phase, sea lions identify the location of prey and gather to encircle it. Within the algorithm, the prey's location is analogous to the best current solution found so far. To simulate this behavior, the positions of the sea lions are updated using the following equation:

$$X^{i+1} = X_{best}^{i} - C \mid 2 \cdot r \cdot X_{best}^{i} - X^{i} \mid \quad (4)$$

In this equation, X^{i+1} denotes the new position of the search agent after the update, X_{best}^{i} is the position vector of the best solution, and X^{i} represents the sea lion's position in the current iteration i. The variable C decreases linearly from 2 to 0 throughout the iterations, and r is a random value within the range [0, 1].

Step 3 Vocalization Phase: Sea lions use vocalization to communicate and coordinate their hunting activities. To model this, the leader sea lion's behavior is represented by the following equations:

$$\begin{aligned} SP_{(leader)} &= \mid (V_1(1+V_2)) / V_2 \mid \\ V_1 &= sin(\theta) \\ V_2 &= sin(\phi) \end{aligned} \quad (5)$$

Where SP_{leader} is the value that influences the behavior of the sea lion group, and θ and ϕ represent the angles of voice reflection and refraction in the water.

Step 4 Attacking (Exploitation) Phase: Sea lions employ two main techniques to hunt their prey:

- Dwindling encircling: This technique is represented by the value of C in the tracking phase equation, which decreases to shrink the search space around the best solution.
- Circling update: Sea lions chase the bait ball of fishes and hunt them starting from the edges. This behavior is modeled by:

$$X^{i+1} = X_{best} + cos(2\pi m) \mid X_{best} - X^{i} \mid \quad (6)$$

where m is a random number in the range [-1, 1].

Step 5 Searching for Prey (Exploration) Phase: Sea lions also search for new prey in the exploration phase. To simulate this, their positions are updated based on a randomly selected sea lion, using the equation:

$$X^{i+1} = X_{rand}^{i} - C \mid 2 \cdot r \cdot X_{rand}^{i} - X^{i} \mid \quad (7)$$

Here, X_{rand}^{i} represents a randomly selected sea lion from the current population, and r is a random value in the range [0, 1]. Through these steps, the SLO algorithm effectively mimics the hunting behavior of sea lions to explore the search space and find optimal or near-optimal solutions to optimization problems. The flowchart of SLO is illustrated in Figure 3.

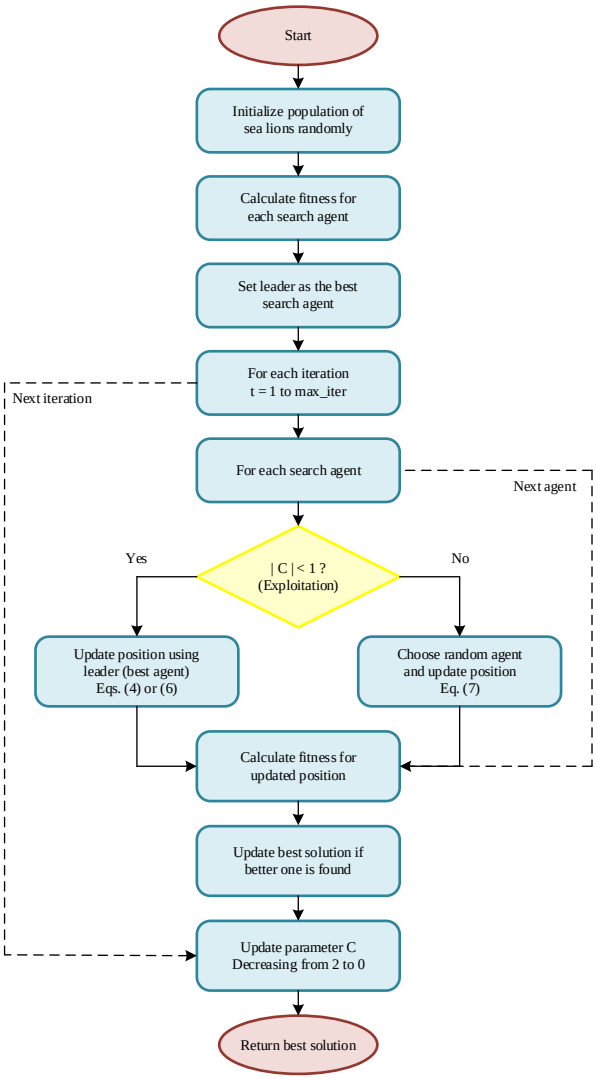

Fig. 3. The flowchart of the utilized SLO.

3.2. Brief Description of The Compared MH-Based SDM Parameter Extraction Methods

This study compares five other MH-based SDM PI approaches. Among them, GA and GWO are well-established MH methods and are therefore not discussed in detail. Ref. [26] proposes a technique based on GA to enhance the accuracy of solar cell parameters extracted. Results indicated low parameter deviation even with large simulated initial errors. The technique was also shown to surpass the quasi-Newton method [26]. Ref. [38] introduces a GWO with dimension learning-based hunting search strategy for extracting parameters of PV cells, focusing on single-diode and double-diode models. The document evaluates I-GWO's performance against numerous algorithms from the literature. In addition to GA and GWO, this study further compares three recently proposed MH methods-AVOA, COA, and GJO-that have been successfully applied to SDM PI problems. The AVOA is a nature-inspired metaheuristic algorithm developed by Abd Elaziz et al. in 2021. It mimics the foraging behavior of African vultures, specifically their search for food and competition. AVOA is characterized by its unique exploration and exploitation strategies, utilizing both the vultures' ability to search over long distances and their competitive feeding behavior to efficiently solve optimization problems [39]. Ref. [40] presents an improved-African vultures optimization algorithm hybridized with the Newton-Raphson method (I-AVO-NR) for estimating parameters of a three-diode PV model. The results demonstrate the algorithm's effectiveness in matching experimental data. The COA, a MH algorithm inspired by coati social behavior, was proposed in 2023 by Dehghani et al. Its key feature is the simulation of cooperative hunting, where some coatis direct prey, and predator evasion. This dual approach enables efficient exploration and exploitation in optimization [41]. Ref. [42] presents the COA for parameter estimation of PV cells. This article selects the COA algorithm for its approach and evaluates its effectiveness using error metrics such as RMSE. This study focuses on optimizing parameters for specific commercial modules including the KC200GT, SW255, and SM55 multi-crystal. The GJO is a MH algorithm inspired by the hunting behavior of golden jackals. Proposed by Chopra et al. in 2022, its key feature is the simulation of a jackal pair's cooperative hunting strategy, encompassing prey searching, encircling, and attacking. This approach with distinct exploration and exploitation phases allows the algorithm to effectively navigate the search space for optimal solutions [43]. Ref. [44] explores the use of the GJO, incorporating non-linear hunting and reinforcement learning, for solar parameter estimation. This study also compares the performance of GJO and its variants against other algorithms for extracting parameters from PV devices, showing detailed I-V data fits and objective function values.

4. The Proposed Improved SLO and Two-Stage SLO

4.1. Improved SLO

The paper proposes an improved version of the SLO algorithm to address the limitations of the original SLO, such as being trapped in local optima and slow convergence. The improved version, called ISLO, incorporates several enhancements to both the exploration and exploitation phases of the algorithm [45].

Inspired by the concept of PSO, this study incorporates the influence of the personal best into the position update formula in the exploration phase to enhance the search capability. This allows the newly created solutions to consider both personal best and the best global solution found so far, promoting a more effective exploration of the search space. Accordingly, Equation (7) is replaced by:

$$X^{i+1} = X^{i} + C \cdot dif_1 + C \cdot dif_2 \tag{8}$$

where:

$$dif_1 = (2r_1 X_{best} - X^{i}), \quad dif_2 = (2r_2 X_{local} - X^{i}) \tag{9}$$

where:

- X^{i}_{local} is the personal best position up to the iteration i.
- r_1, r_2 are random numbers in the range [0, 1].

In the exploitation phase, ISLO employs a bidirectional search strategy to enhance the search process. This involves

generating an opposite solution to the current one and evaluating both to determine the better candidate for the next iteration. The exploitation phase update mechanism is as follows:

$$X^{i+1} = X_{best} + C \cdot N(0,1) \cdot (2r_3 X_{best} - X^i) \quad (10)$$

$$X_{oppo}^{i+1} = LB + UB - X_{best} + r_4 (X_{best} - X^{i+1}) \quad (11)$$

where:

- N (0, 1) is a normal distribution variable.
- LB and UB are the lower and upper bounds of the search space.
- r3, r4 are random numbers in the range of [0, 1].

Additionally, ISLO employs the Lévy flight to introduce a more complex trajectory for the sea lions, further enhancing the diversity and local exploitation ability of the algorithm. The position update formula using Lévy flight is given by Eq. (12), which is primarily designed to complement Eq. (6). In this study, the sea lion selects either the circling update (Eq. (6)) or the Lévy flight update (Eq. (12)) with equal probability to calculate the attack position.

$$X^{i+1} = X_{best} + ss \cdot Levy(s) \otimes (X_{best} - X^i) \quad (12)$$

where:

- ss is the step size.
- $\otimes$ is entry-wise multiplications.
- Lévy(s) is a set of Lévy step lengths in a D-dimensional space.

4.2. Two-stage SLO

To further enhance the parameter identification performance of the proposed approach, this study introduces a two-stage SLO PI method. The main concept is to utilize the known mathematical relationships of the SDM to calculate initial parameter values based on basic information provided in the datasheet. Although the calculated parameters are not perfectly accurate, they can serve as valuable references for the second-stage MH method. Ref. [46] suggest that SDM parameters can be identified using manufacturer datasheet values-such as open-circuit voltage, short-circuit current, and maximum power point data-combined with temperature coefficients through analytical methods. Based on this concept, the initial estimates for the five parameters to be identified are derived as follows:

First, under short-circuit conditions, the photocurrent I_{ph} is approximately equal to the short-circuit current, leading to:

$$I_{ph0} = I_{sc} \quad (13)$$

The initial value of saturation current Is0 can be calculated as the following equation based on basic semiconductor physics.

$$I_{s0} = C_0 \cdot T_0^3 \cdot exp\left(-\frac{E_i}{k \cdot T_0}\right) \quad (14)$$

- I_{s0}: Diode saturation current at the reference temperature T_0.
- C_0: Constant, representing the cell technology-specific scaling factor.
- T_0: Reference temperature (usually 25°C or 298 K).
- E_g: Bandgap energy of semiconductor material (e.g., silicon ~1.12 eV).
- k: Boltzmann constant ($8.617333262 \times 10^{-5}$ eV/K).

Next, the initial value of the ideality factor can be estimated from the open-circuit voltage, as follows. Since at open-circuit, current $I=0$, and voltage is $V=V_{oc0}$, substituting into the SDM and rearrange yield:

$$I_{ph} = I_s \left[exp\left(\frac{V_{oc0}}{nV_t}\right) - 1 \right] \quad (15)$$

Since $I_{ph} \approx I_{sc0}$ at STC, take natural logarithm on both sides, n0 can be obtained as:

$$n_0 = \frac{V_{oc0}}{V_t \cdot ln\left(\frac{I_{sc0}}{I_s} + 1\right)} \quad (16)$$

rewrite the MPP equation in the following form to isolate the exponential term by neglecting R_{h0}, Eq. (17) can be obtained.

$$I_{ph0} - I_{mpp} = I_{s0} \left[exp\left(\frac{V_{mpp} + I_{mpp} R_{s0}}{n_0 V_t}\right) - 1 \right] \quad (17)$$

Take logarithm and solve for R_{s0} yield;

$$R_{s0} = \frac{n_0 V_t \cdot ln\left(\frac{I_{ph0} - I_{mpp}}{I_{s0}} + 1\right) - V_{mpp}}{I_{mpp}} \quad (18)$$

Finally, the initial value of R_{h0} can be calculated by rearranging the full SDM equation (including shunt resistance) at the MPP point.

$$I_{mpp} = I_{ph0} - I_{s0}\left[exp(x) - 1\right] - \frac{x \cdot n_0 V_t}{R_{h0}} \quad (19)$$

where:

$$x = \frac{V_{mpp} + I_{mpp} R_{s0}}{n_0 V_t} \quad (20)$$

Rearrange to solve for R_{h0} yield

$$R_{h0} = \frac{x \cdot n_0 V_t}{I_{ph0} - I_{mpp} - I_{s0}(exp(x) - 1)} \quad (21)$$

After calculating the initial estimates of the SDM parameters using Eqs. (13), (14), (16), (18), (21), each value is multiplied by an upper bound coefficient (UB) to define the upper limit of the ISLO particle search range, and by a lower bound coefficient (LB) to define the lower limit. ISLO optimization can then be performed. Since this method modifies only the search range without altering the update equations of the algorithm, the proposed two-stage approach can be applied to any MH algorithm. In this study, this concept is also extended to all implemented algorithms for comparative analysis. The UB and LB values are set to 2 and 0.5 in this study, respectively. The flowchart of the proposed two-stage ISLO is illustrated in Figure 4.

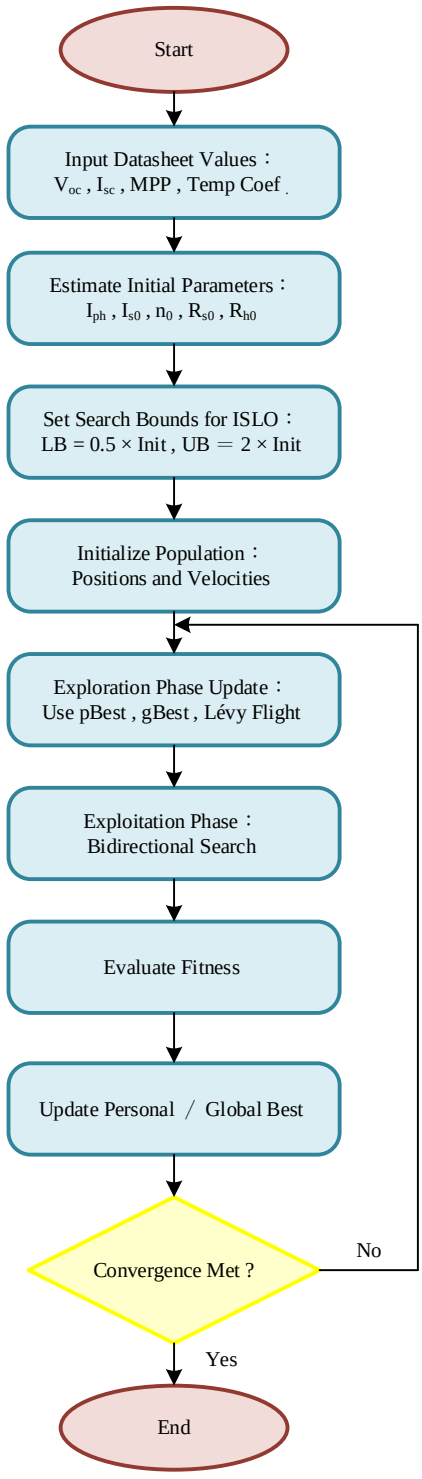

Fig. 4. The flowchart of the proposed two-stage ISLO.

5. Simulation and Experimental Results

This study implements the proposed ISLO, the two-stage ISLO, and five MH algorithms previously applied to SDM PI problems in the literature. The simulations were conducted using Python in a Jupyter Notebook environment, on a computer with an Intel Core i7-12700 processor and 16GB of RAM.

The performance of these methods is validated using the I-V curve of a commercial solar module. Specifically, the GSM5-72-210 solar module manufactured by GermanSolar is used, with its specifications summarized in Table 2. The investigation focuses on the impact of epoch number, particle number, and initialization methods.

Figure 5 illustrates the convergence trends of various MH methods with a particle number of 100, epoch of 1000, and initialization using the conventional random method. As shown in Figure 5, the methods achieving the lowest final fitness values are ISLO, SLO, and GWO, respectively.

Figures 6 and 7 present a comparative analysis of relative parameter errors and error distributions for various algorithms applied to the SDM parameter estimation, including SLO, Improved SLO (ISLO), COA, AVOA, GJO, GA, and GWO. Figure 6 displays box plots of relative errors for parameters I_{ph0}, n_0, I_0, R_{h0}, and R_{s0}, highlighting ISLO's superior performance. ISLO consistently exhibits lower median errors and reduced variability compared to other methods, notably outperforming SLO, GA, and GWO across all parameters. For instance, ISLO shows significantly smaller errors in R_{s0} (close to 0%) compared to the higher deviations in GWO and GA.

Figure 7 complements this with histograms of error distributions, reinforcing ISLO's advantage. The error distributions for ISLO are narrower and more centered around zero, indicating higher precision and stability. In contrast, methods like GWO and GA display wider distributions with larger errors, especially for R_{h0} and R_{s0}. The incorporation of Lévy flight and personal best information in ISLO reduces the RMSE by 59.7% compared to SLO, and the two-stage framework further enhances accuracy, achieving 89.6% and 91.3% improvements in mean and standard deviation of RMSE. This underscores ISLO's effectiveness and robustness, setting it apart from other algorithms in both accuracy and reliability.

Similarly, Figures 8-10 depict the results obtained by setting the search range using the two-stage method.

Table 2. Specifications of solar cells used in this study

Item	Single PV Module
Maximum Power (P_{max}) (W)	210
Open-Circuit Voltage (V_{oc}) (V)	45.72
Short-Circuit Current (I_{sc}) (A)	5.77
Voltage at Maximum Power Point (V_{MPP}) (V)	38.52
Current at Maximum Power Point (I_{MPP}) (A)	5.45
Temperature Coefficient of Open-Circuit Voltage (β_{Voc}) (%/°C)	-0.331
Temperature Coefficient of Short-Circuit Current (α_{Isc}) (%/°C)	0.059

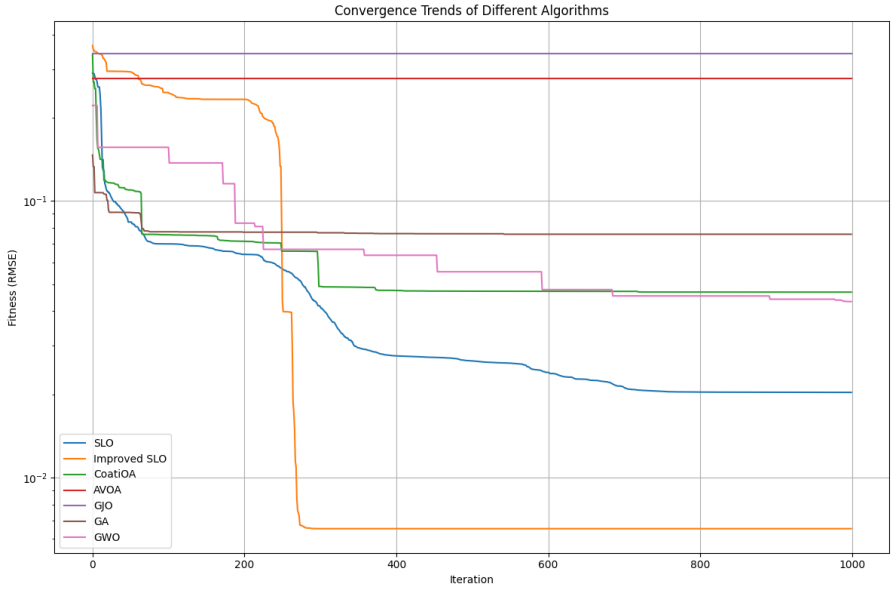

Fig. 5. Convergence trends of various MH methods under random initialization conditions.

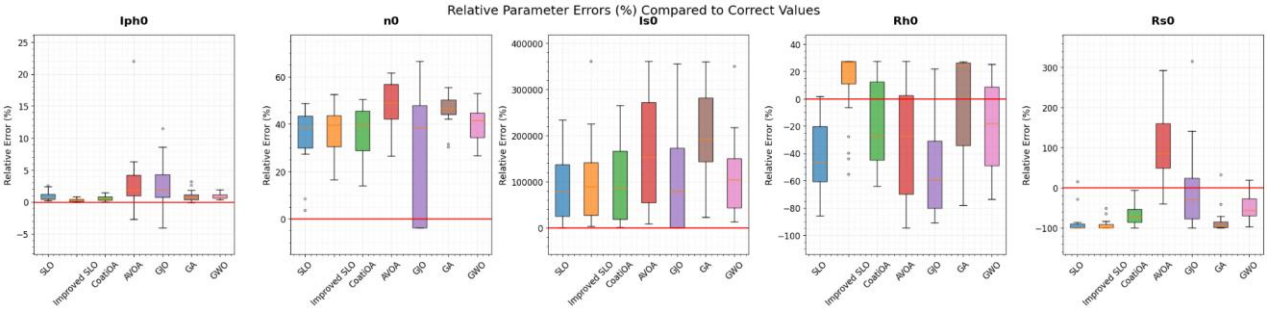

Fig. 6. Box plot of relative errors for parameter estimation results of various MH methods under random initialization conditions.

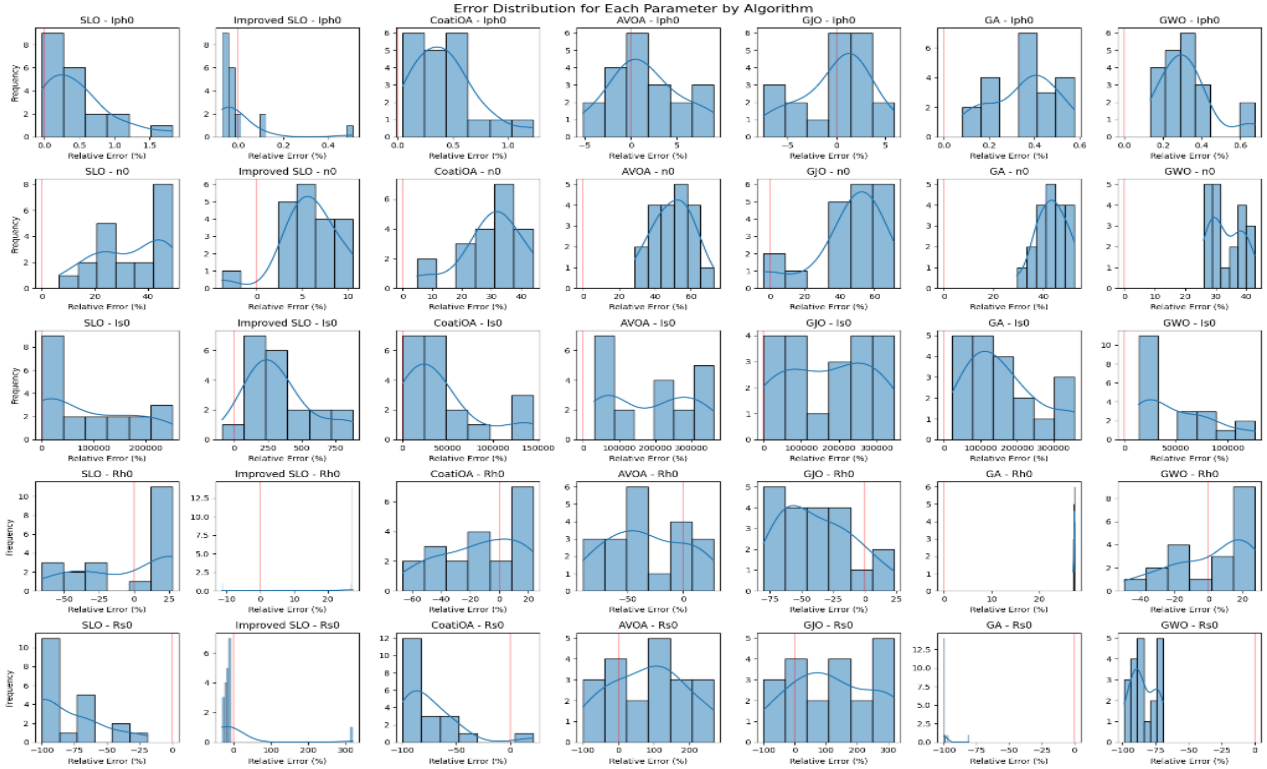

Fig. 7. Distribution plot of relative errors for parameter estimation results of various MH methods under random initialization conditions.

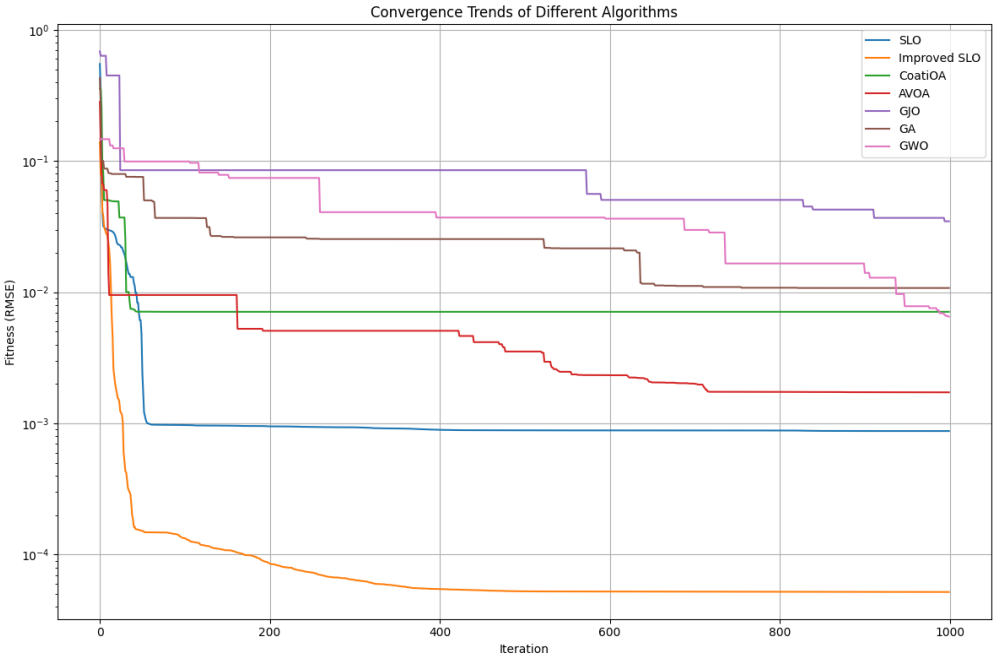

Fig. 8. Convergence trends of various MH methods under two-stage initialization conditions.

Figures 9 and 10 illustrate the impact of a two-stage approach on parameter estimation for the SDM. In the first stage, the method leverages the physical behavior of SDM to estimate initial particle ranges (solution space), followed by the original algorithms in the second stage. Figure 9 shows box plots of relative parameter errors (I_{ph0}, n_0, I_0, R_{h0}, and R_{s0}), while Figure 10 provides error distribution histograms. ISLO continues to outperform all other methods, exhibiting the lowest median errors and tightest interquartile ranges, especially for R_{s0} and R_{h0}, where its errors are minimal compared to the broader deviations in GWO and GA. The two-stage approach benefits all algorithms, with noticeable reductions in error variability and shifts toward zero. For instance, ISLO's error distributions in Figure 10 are significantly narrower and more centered, reflecting its enhanced precision, while other methods like COA and AVOA also show improved stability. This dual-stage strategy, by refining initial conditions, uniformly enhances the accuracy and robustness of all algorithms, with ISLO maintaining its lead due to its integrated Lévy flight and personal best enhancements.

Table 3 and Table 4 present a comparative analysis of several metaheuristic optimization algorithms, evaluating their performance based on RMSE and MAE across varying particle numbers and epochs. The results are segregated into two categories: the first (Table 3) employs a traditional random initialization with a broader parameter range, while the second (Table 4) leverages a preliminary estimation of parameters derived from the SDM to refine the search space.

A critical observation is the significant influence of the initialization strategy on the final RMSE/MAE. The data clearly indicates that utilizing the SDM-derived parameter estimates for initialization consistently yields superior results compared to random initialization. Specifically, across all particle and epoch configurations, the Mean RMSE/MAE values are substantially lower when using the SDM-informed initialization. This highlights the importance of a well-informed initial search space, as it facilitates faster convergence and improved solution accuracy. Random initialization, conversely, often leads to higher RMSE/MAE values, suggesting that the algorithms struggle to efficiently navigate the larger, less refined search space.

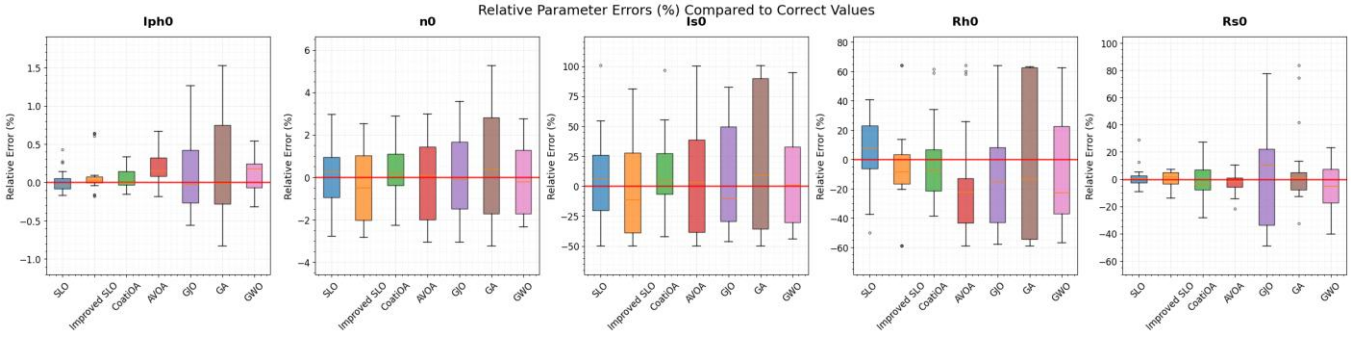

Fig. 9. Box plot of relative errors for parameter estimation results of various MH methods under two-stage initialization conditions.

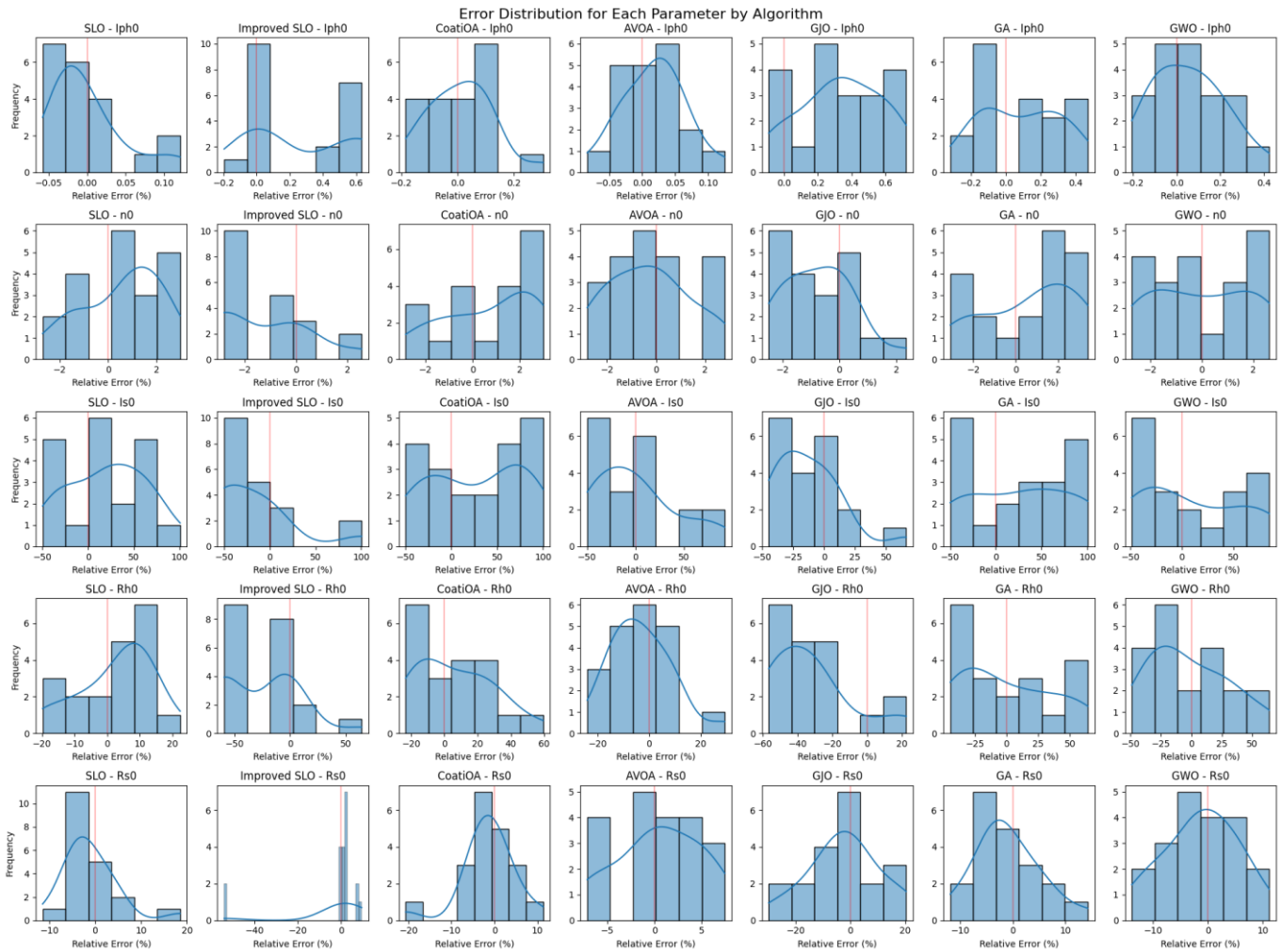

Fig. 10. Distribution plot of relative errors for parameter estimation results of various MH methods under two-stage initialization conditions.

Table 3. Random initialization results (Mean (Std Dev))

Algorithm	Particle=10, Epoch=10		Particle=50, Epoch=50		Particle=50, Epoch=100		Particle=100, Epoch=100		Particle=100, Epoch=1000	
	RMSE	MAE	RMSE	MAE	RMSE	MAE	RMSE	MAE	RMSE	MAE
SLO	0.3095 (0.1422)	0.197 (0.125)	0.0925 (0.0431)	0.056 (0.019)	0.0727 (0.0640)	0.056 (0.021)	0.0662 (0.0294)	0.046 (0.019)	0.0452 (0.0210)	0.036 (0.015)
ISLO	0.2967 (0.0572)	0.271 (0.153)	0.0840 (0.0330)	0.055 (0.030)	0.0660 (0.0284)	0.041 (0.013)	0.0568 (0.0194)	0.034 (0.012)	0.0182 (0.0115)	0.005 (0.003)
COA	0.2651 (0.1501)	0.168 (0.042)	0.1109 (0.0775)	0.076 (0.031)	0.0844 (0.0303)	0.054 (0.019)	0.0765 (0.0447)	0.047 (0.018)	0.0432 (0.0494)	0.032 (0.008)
AVOA	0.7389 (0.2966)	0.555 (0.287)	0.4399 (0.2319)	0.311 (0.123)	0.4338 (0.1908)	0.265 (0.159)	0.3935 (0.1336)	0.229 (0.119)	0.3689 (0.1726)	0.237 (0.102)
GJO	0.5377 (0.2058)	0.391 (0.329)	0.2826 (0.1711)	0.237 (0.194)	0.2824 (0.1964)	0.231 (0.169)	0.3487 (0.2155)	0.187 (0.153)	0.3745 (0.1408)	0.348 (0.123)
GA	0.6647 (0.2286)	0.446 (0.236)	0.1419 (0.0400)	0.099 (0.027)	0.1188 (0.0470)	0.093 (0.031)	0.0742 (0.0156)	0.061 (0.024)	0.0564 (0.0128)	0.094 (0.010)
GWO	0.2578 (0.0744)	0.140 (0.037)	0.1434 (0.0460)	0.104 (0.024)	0.1163 (0.0312)	0.084 (0.023)	0.0935 (0.0251)	0.063 (0.015)	0.0417 (0.0072)	0.031 (0.007)

Table 4. Analytical formula initialization results (Mean (Std Dev))

Algorithm	Particle=10, Epoch=10		Particle=50, Epoch=50		Particle=50, Epoch=100		Particle=100, Epoch=100		Particle=100, Epoch=1000	
	RMSE	MAE	RMSE	MAE	RMSE	MAE	RMSE	MAE	RMSE	MAE
SLO	0.3914 (0.2790)	0.331 (0.237)	0.0192 (0.0144)	0.021 (0.010)	0.0175 (0.0095)	0.015 (0.010)	0.0098 (0.0130)	0.007 (0.006)	0.0024 (0.0027)	0.002 (0.001)
ISLO	0.3852 (0.2538)	0.377 (0.244)	0.0144 (0.0141)	0.013 (0.010)	0.0143 (0.0093)	0.009 (0.009)	0.0080 (0.0049)	0.004 (0.004)	0.0019 (0.0010)	0.001 (0.001)
COA	0.2086 (0.2182)	0.136 (0.137)	0.0223 (0.0212)	0.017 (0.007)	0.0206 (0.0209)	0.019 (0.009)	0.0153 (0.0080)	0.011 (0.007)	0.0070 (0.0042)	0.006 (0.004)
AVOA	0.4556 (0.2840)	0.305 (0.262)	0.0378 (0.0227)	0.010 (0.013)	0.0176 (0.0116)	0.010 (0.011)	0.0146 (0.0275)	0.005 (0.006)	0.0120 (0.0150)	0.006 (0.009)
GJO	0.6826 (0.2452)	0.385 (0.219)	0.0485 (0.0171)	0.027 (0.016)	0.0403 (0.0130)	0.024 (0.009)	0.0345 (0.0200)	0.028 (0.013)	0.0207 (0.0084)	0.016 (0.007)
GA	0.8411 (0.2741)	0.525 (0.303)	0.0643 (0.0503)	0.046 (0.027)	0.0472 (0.0360)	0.024 (0.017)	0.0263 (0.0207)	0.022 (0.016)	0.0104 (0.0094)	0.006 (0.003)
GWO	0.3045 (0.3395)	0.224 (0.181)	0.0410 (0.0209)	0.012 (0.008)	0.0304 (0.0186)	0.009 (0.007)	0.0128 (0.0067)	0.008 (0.004)	0.0056 (0.0027)	0.005 (0.002)

The tables also demonstrate the impact of particle and epoch numbers on algorithm performance. Generally, increasing both the number of particles and the number of epochs leads to a reduction in RMSE/MAE, indicating improved solution quality. For instance, with SDM-informed initialization, increasing the particle number from 10 to 100, while maintaining 100 epochs, significantly reduces the Mean RMSE/MAE for all algorithms. Similarly, holding the particle number at 100 and increasing the epochs from 100 to 1000 further refines the results. This trend is consistent with the fundamental principles of metaheuristic optimization: a larger population allows for broader exploration of the search space, and more iterations provide additional opportunities for convergence towards the optimum.

While the initialization strategy and parameter settings exert a dominant influence, the relative performance of the algorithms also warrants attention. ISLO consistently demonstrates strong performance, often achieving the lowest RMSE/MAE values, particularly with SDM-informed initialization and higher particle/epoch numbers. This suggests that the enhancements incorporated into ISLO, such as personal best information, Lévy flight calculation, and di-directional search, effectively contribute to its optimization capabilities. Algorithms like AVOA and GWO, on the other hand, generally exhibit higher RMSE/MAE values, indicating potentially less efficient search mechanisms for this specific problem.

In conclusion, the results underscore the critical role of informed initialization in metaheuristic optimization. Utilizing problem-specific knowledge to constrain the search space can significantly enhance the efficiency and accuracy of these algorithms. Furthermore, increasing particle and epoch numbers generally improves performance, albeit at a higher computational cost. Finally, the ISLO algorithm demonstrates promising results, suggesting that its enhanced search strategies offer advantages in terms of convergence and solution quality.

Finally, Figure 11 presents a comparison between the I-V curves derived from the five parameters obtained by various MH methods (with a particle number of 100 and epoch number of 1000) using two different initialization methods and the actual I-V curve, based on the SDM. As shown in Figure 11, with the conventional random initialization method, even with the epoch number set to 1000, only a few MH methods produce I-V curves that closely match the actual values. However, when the two-stage initialization method is employed to narrow the search range, nearly all MH methods yield I-V curves that effectively align with the actual values, thereby validating the effectiveness of the proposed two-stage method.

6. Conclusion and Recommendations

This study presents a two-stage metaheuristic framework for improved parameter identification in the SDM. It introduces the SLO algorithm for SDM parameter estimation, a novel application that outperforms established algorithms such as GA, GWO, COA, AVOA, and GJO. Additionally, an Improved SLO, incorporating Lévy flight and personal best information, enhances estimation accuracy, achieving a 59.7% reduction in RMSE compared to the original SLO.

The proposed two-stage ISLO framework further improves precision and stability, yielding 89.6% and 91.3% reductions in the mean and standard deviation of RMSE, respectively, compared to ISLO with random initialization. These results demonstrate the effectiveness and reliability of the proposed ISLO algorithm and two-stage methodology for accurate PV model parameter identification.

For future work, the proposed framework could be extended to real-time applications, such as online parameter estimation for PV systems under varying environmental conditions. Additionally, adapting the methodology to multi-diode models, such as the DDM or TDM, may enhance its applicability to more complex PV systems. Integration with embedded systems for efficient on-device implementation could further increase the practical value of this approach, enabling its use in resource-constrained environments.

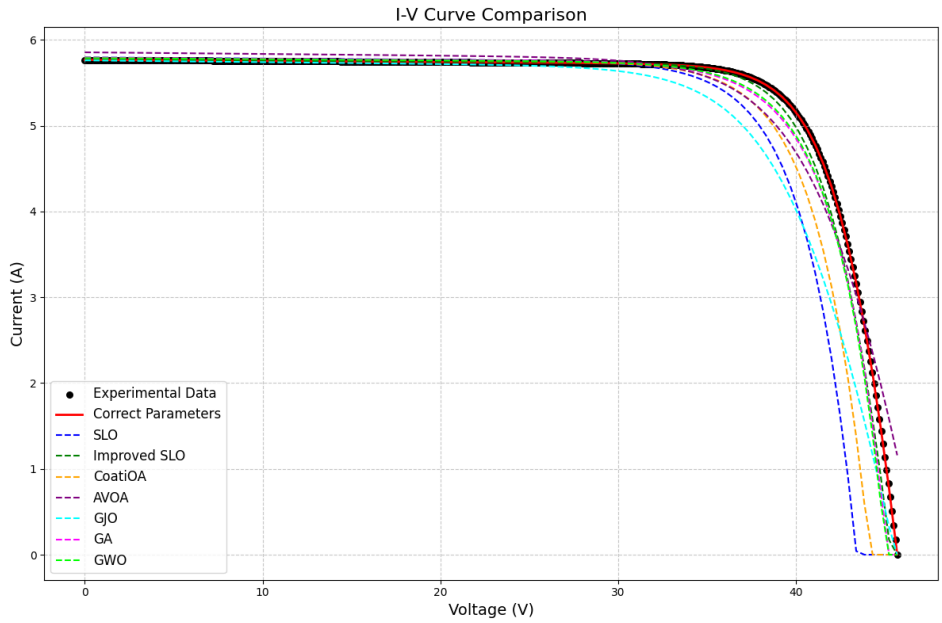

(a)

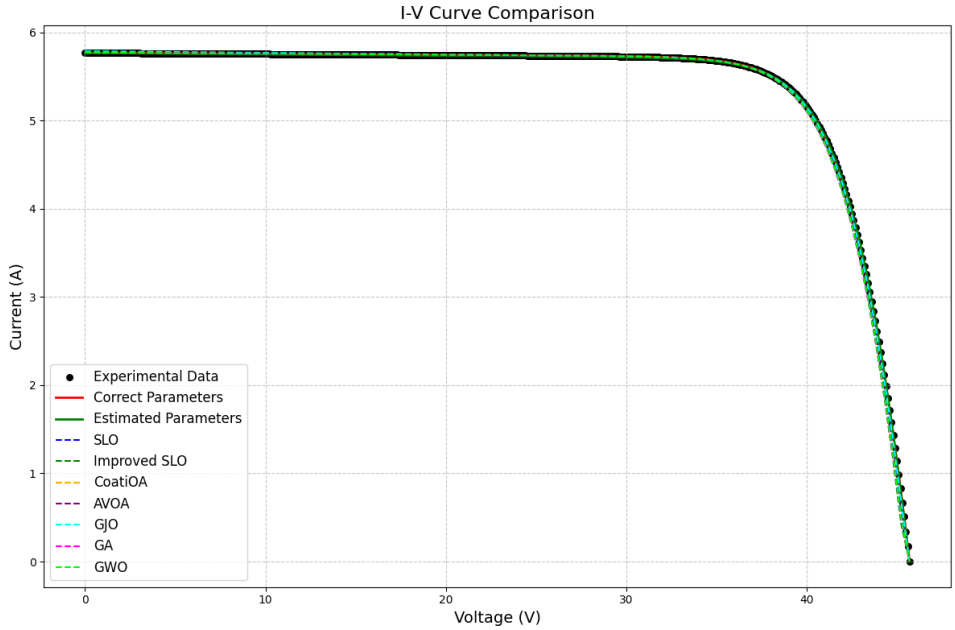

(b)

Fig. 11. Comparison of I-V curves for two different initialization methods: (a) random initialization, (b) two-stage initialization

References

[1] I. S. Rad, M. Alinezhad, S. E. Naghibi, M. A. Kamarposhti, "Detection of internal fault in differential transformer protection based on fuzzy method", International Journal of Physical Sciences, vol. 6, No. 26, pp. 6150-6158, 2011, Doi: 10.5897/IJPS11.478.

[2] I. A. Joneidi, M. A. Kamarposhti, A. A. Shayegani Akmal, H. Mohseni, "Leakage current analysis, FFT calculation and electric field distribution under water droplet on polluted silicon rubber insulator", Electrical Engineering, vol. 95, pp. 315-323, 2013, Doi: 10.1007/s00202-012-0260-8.

[3] V. L. Brano, A. Orioli, G. Ciulla, A. Di Gangi, "An improved five-parameter model for photovoltaic modules", Solar Energy Materials and Solar Cells, vol. 94, pp. 1358-1370, 2010, Doi: 10.1016/j.solmat.2010.04.003.

[4] A. Orioli, A. Di Gangi, "A procedure to calculate the five-parameter model of crystalline silicon photovoltaic

modules on the basis of the tabular performance data", Applied Energy, vol. 102, pp. 1160-1177, 2013, Doi: 10.1016/j.apenergy.2012.06.036.

[5] S. Lineykin, M. Averbukh, A. Kuperman, "An improved approach to extract the single-diode equivalent circuit parameters of a photovoltaic cell/panel", Renewable and Sustainable Energy Reviews, vol. 30, pp. 282-289, 2014, Doi: 10.1016/j.rser.2013.10.015.

[6] M. Calasan, S. H. E. A. Aleem, A. F. Zobaa, "A new approach for parameters estimation of double and triple diode models of photovoltaic cells based on iterative Lambert W function", Solar Energy, vol. 218, pp. 392-412, 2021, Doi: 10.1016/j.solener.2021.02.038.

[7] M. Calasan, M. Al-Dhaifallah, Z. M. Ali, S. H. E. A. Aleem, "Comparative analysis of different iterative methods for solving current-voltage characteristics of double and triple diode models of solar cells", Mathematics, vol. 10, p. 3082, 2022, Doi: 10.3390/math10173082.

[8] E. A. Silva, F. Bradaschia, M. C. Cavalcanti, A. J. Nascimento, "Parameter estimation method to improve the accuracy of photovoltaic electrical model", IEEE Journal of Photovoltaics, vol. 6, pp. 278-285, 2016, Doi: 10.1109/JPHOTOV.2015.2483369.

[9] M. H. Qais, H. M. Hasanien, S. Alghuwainem, K. H. Loo, M. A. Elgendy, R. A. Turky, "Accurate three-diode model estimation of photovoltaic modules using a novel circle search algorithm", Ain Shams Engineering Journal, vol. 13, p. 101824, 2022, Doi: 10.1016/j.asej.2022.101824.

[10] M. A. Soliman, A. Al-Durra, H. M. Hasanien, "Electrical parameters identification of three-diode photovoltaic model based on equilibrium optimizer algorithm", IEEE Access, vol. 9, pp. 41891-41901, 2021, Doi: 10.1109/ACCESS.2021.3065386.

[11] M. Gafar, R. A. El-Sehiemy, H. M. Hasanien, A. Abaza, "Optimal parameter estimation of three solar cell models using modified spotted hyena optimization", Journal of Ambient Intelligence and Humanized Computing, vol. 15, pp. 361-372, 2022, Doi: 10.1007/s12652-022-03896-9.

[12] F. M. Makahleh, A. Amer, A. A. Manasrah, H. Attar, A. A. Solyman, M. A. Kamarposhti, P. Thounthong, "Optimal management of energy storage systems for peak shaving in a smart grid", Computer Modeling in Engineering and Sciences, vol. 75, No. 2, pp. 3317-3337, 2023, Doi: 10.32604/cmc.2023.035690.

[13] M. Mojtahedzadeh Larijani, M. Ahmadi Kamarposhti, T. Nouri, "Stochastic unit commitment study in a power system with flexible load in presence of high penetration renewable farms", International Journal of Energy Research, vol. 2023, No. 1, article ID 9979610, 2023, Doi: 10.1155/2023/9979610.

[14] E. Eslami, M. Ahmadi Kamarposhti, "Optimal design of solar–wind hybrid system-connected to the network with cost-saving approach and improved network reliability index", SN Applied Sciences, vol. 1, No. 12, article 1742, 2019, Doi: 10.1007/s42452-019-1710-y.

[15] M. A. Kamarposhti, S. M. M. Khormandichali, A. A. A. Solyman, "Locating and sizing of capacitor banks and multiple DGs in distribution system to improve reliability indexes and reduce loss using ABC algorithm", Bulletin of Electrical Engineering and Informatics, vol. 10, No. 2, pp. 559-568, 2021, Doi: 10.11591/eei.v10i2.2641.

[16] M. Ahmadi Kamarposhti, H. Shokouhandeh, Y. Gholami Omali, I. Colak, P. Thounthong, W. Holderbaum, "Optimal coordination of TCSC and PSS2B controllers in electric power systems using MOPSO multiobjective algorithm", International Transactions on Electrical Energy Systems, vol. 2022, No. 1, article ID 5233620, 2022, Doi: 10.1155/2022/5233620.

[17] M. A. Kamarposhti, I. Colak, H. Shokouhandeh, C. Iwendi, S. Padmanaban, S. S. Band, "Optimum operation management of microgrids with cost and environment pollution reduction approach considering uncertainty using multi-objective NSGAII algorithm", IET Renewable Power Generation, vol. 19, No. 1, article e12579, 2025, Doi: 10.1049/rpg2.12579.

[18] K. Ishaque, Z. Salam, "An improved modeling method to determine the model parameters of photovoltaic (PV) modules using differential evolution (DE)", Solar Energy, vol. 85, pp. 2349-2359, 2011, Doi: 10.1016/j.solener.2011.06.025.

[19] K. Ishaque, Z. Salam, H. Taheri, A. Shamsudin, "A critical evaluation of EA computational methods for photovoltaic cell parameter extraction based on two diode model", Solar Energy, vol. 85, pp. 1768-1779, 2011, Doi: 10.1016/j.solener.2011.04.015.

[20] K. Ishaque, Z. Salam, S. Mekhilef, A. Shamsudin, "Parameter extraction of solar photovoltaic modules using penalty-based differential evolution", Applied Energy, vol. 99, pp. 297-308, 2012, Doi: 10.1016/j.apenergy.2012.05.017.

[21] M. Ye, X. Wang, Y. Xu, "Parameter extraction of solar cells using particle swarm optimization", Journal of Applied Physics, vol. 105, p. 094502, 2009, Doi: 10.1063/1.3122082.

[22] H. Hengsi, J. W. Kimball, "Parameter determination of photovoltaic cells from field testing data using particle swarm optimization", IEEE Power and Energy Conference at Illinois, Urbana, IL, USA, pp. 1-6, 25-26 February 2011, Doi: 10.1109/PECI.2011.5740496.

[23] J. J. Soon, K.-S. Low, "Photovoltaic model identification using particle swarm optimization with inverse barrier constraint", IEEE Transactions on Power Electronics, vol. 27, pp. 3975-3983, 2012, Doi: 10.1109/TPEL.2012.2188818.

[24] M. Zagrouba, A. Sellami, M. Bouaïcha, M. Ksouri, "Identification of PV solar cells and modules parameters using the genetic algorithms: Application to maximum

power extraction", Solar Energy, vol. 84, pp. 860-866, 2010, Doi: 10.1016/j.solener.2010.02.012.

[25] A. Sellami, M. Bouaïcha, "Application of the genetic algorithms for identifying the electrical parameters of PV solar generators", Solar Cells – Silicon Wafer-Based Technologies, A. Kosyachenko, Ed., London: InTech Open, 2011, pp. 349-364, Doi: 10.5772/22714.

[26] J. A. Jervase, H. Bourdoucen, A. Al-Lawati, "Solar cell parameter extraction using genetic algorithms", Measurement Science and Technology, vol. 12, p. 1922, 2001, Doi: 10.1088/0957-0233/12/11/322.

[27] A. Askarzadeh, A. Rezazadeh, "Artificial bee swarm optimization algorithm for parameters identification of solar cell models", Applied Energy, vol. 102, pp. 943-949, 2013, Doi: 10.1016/j.apenergy.2012.09.052.

[28] M. Ketkar, A. M. Chopde, "Efficient parameter extraction of solar cell using modified ABC", International Journal of Computer Applications, vol. 102, pp. 1-6, 2014, Doi: 10.5120/17776-8535.

[29] D. Oliva, E. Cuevas, G. Pajares, "Parameter identification of solar cells using artificial bee colony optimization", Energy, vol. 72, pp. 93-102, 2014, Doi: 10.1016/j.energy.2014.05.011.

[30] D. Oliva, M. A. Aziz, A. Hassanien, "Parameter estimation of photovoltaic cells using an improved chaotic whale optimization algorithm", Applied Energy, vol. 200, pp. 154-174, 2017, Doi: 10.1016/j.apenergy.2017.05.029.

[31] M. A. Elaziz, D. Oliva, "Parameter estimation of solar cells diode models by an improved opposition-based whale optimization algorithm", Energy Conversion and Management, vol. 171, pp. 1843-1859, 2018, Doi: 10.1016/j.enconman.2018.05.062.

[32] G. Xiong, J. Zhang, X. Yuan, D. Shi, Y. He, G. Yao, "Parameter extraction of solar photovoltaic models by means of a hybrid differential evolution with whale optimization algorithm", Solar Energy, vol. 176, pp. 742-761, 2018, Doi: 10.1016/j.solener.2018.10.050.

[33] X. Lin, Y. Wu, "Parameters identification of photovoltaic models using niche-based particle swarm optimization in parallel computing architecture", Energy, vol. 196, p. 117054, 2020, Doi: 10.1016/j.energy.2020.117054.

[34] M. H. Qais, H. M. Hasanien, S. Alghuwainem, "Parameters extraction of three-diode photovoltaic model using computation and Harris Hawks optimization", Energy, vol. 195, p. 117040, 2020, Doi: 10.1016/j.energy.2020.117040.

[35] M. A. Soliman, H. M. Hasanien, A. Alkuhayli, "Marine predators algorithm for parameters identification of triple-diode photovoltaic models", IEEE Access, vol. 8, pp. 155832-155842, 2020, Doi: 10.1109/ACCESS.2020.3019244.

[36] M. Abdel-Basset, D. Sl-Shahat, R. K. Chakraborty, M. Ryan, "Parameter estimation of photovoltaic models using an improved marine predators algorithm", Energy Conversion and Management, vol. 227, p. 113491, 2021, Doi: 10.1016/j.enconman.2020.113491.

[37] R. Masadeh, B. A. Mahafzah, A. Sharieh, "Sea lion optimization algorithm", International Journal of Advanced Computer Science and Applications, vol. 10, No. 5, 2019, Doi: 10.14569/IJACSA.2019.0100548.

[38] H. Rezaei, O. Bozorg-Haddad, X. Chu, "Grey wolf optimization (GWO) algorithm", Advanced Optimization by Nature-Inspired Algorithms, Singapore: Springer, 2017, pp. 81-91, Doi: 10.1007/978-981-10-5221-7_9.

[39] B. Abdollahzadeh, F. S. Gharehchopogh, S. Mirjalili, "African vultures optimization algorithm: A new nature-inspired metaheuristic algorithm for global optimization problems", Computers and Industrial Engineering, vol. 158, p. 107408, 2021, Doi: 10.1016/j.cie.2021.107408.

[40] C. Kumar, D. M. Mary, "Parameter estimation of three-diode solar photovoltaic model using an improved African vultures optimization algorithm with Newton–Raphson method", Journal of Computational Electronics, vol. 20, pp. 2563-2593, 2021, Doi: 10.1007/s10825-021-01812-6.

[41] M. Dehghani, Z. Montazeri, E. Trojovská, P. Trojovský, "Coati optimization algorithm: A new bio-inspired metaheuristic algorithm for solving optimization problems", Knowledge-Based Systems, vol. 259, p. 110011, 2023, Doi: 10.1016/j.knosys.2022.110011.

[42] R. Elshara, A. Hançerlioğullari, J. Rahebi, J. M. Lopez-Guede, "PV cells and modules parameter estimation using coati optimization algorithm", Energies, vol. 17, No. 7, p. 1716, 2024, Doi: 10.3390/en17071716.

[43] N. Chopra, M. M. Ansari, "Golden jackal optimization: A novel nature-inspired optimizer for engineering applications", Expert Systems with Applications, vol. 198, p. 116924, 2022, Doi: 10.1016/j.eswa.2022.116924.

[44] C. S. Sundar Ganesh, C. Kumar, M. Premkumar, B. Derebew, "Enhancing photovoltaic parameter estimation: Integration of non-linear hunting and reinforcement learning strategies with golden jackal optimizer", Scientific Reports, vol. 14, No. 1, p. 2756, 2024, Doi: 10.1038/s41598-024-52670-8.

[45] B. M. Nguyen, T. Tran, T. Nguyen, G. Nguyen, "An improved sea lion optimization for workload elasticity prediction with neural networks", International Journal of Computational Intelligence Systems, vol. 15, No. 1, p. 90, 2022, Doi: 10.1007/s44196-022-00156-8.

[46] M. Hejri, H. Mokhtari, "On the comprehensive parametrization of the photovoltaic (PV) cells and modules", IEEE Journal of Photovoltaics, vol. 7, No. 1, pp. 250-258, 2016, Doi: 10.1109/JPHOTOV.2016.2617038.